HiSST: 2nd International Conference on
High-Speed Vehicle Science Technology
11–15 September 2022, Bruges, Belgium

Jet noise of an airframe-integrated dual-mode nozzle propulsion system during take-off and landing

Karel H. Lammers[1], Remco Habing[2], Guillaume Grossir[3], Christophe Schram[4]

Abstract

This paper describes the application of existing semi-empirical jet noise models to flows expected in airframe-integrated propulsion systems. In this study, the LAPCAT-MR2.4 air-breathing propulsion system for hypersonic aviation is examined during the subsonic landing and take-off (LTO) cycle. For this part of the flight envelope the internal flow topology is that of a subsonic core flow in the main nozzle, which is penetrated by two lateral jets with low-supersonic discharge velocities. The complex three-dimensional mixing between the subsonic and supersonic streams takes place within a long diffuser nozzle that is also integrated within the airframe. During the LTO cycle it shields the jet and offers room for acoustic liners to reduce noise emissions. In this research the propulsion system of the LAPCAT-MR2.4 vehicle is represented by a simplified coaxial axi-symmetric configuration, still retaining the key flow features of the real geometry, which are considered to be aero-acoustically dominant. A scaled-down nozzle for an unheated jet is designed, instrumented and tested in order to evaluate the applicability of using existing semi-empirical jet noise models to predict the far field noise arising from this type of propulsion systems. With these insights, key jet noise sources and directivities were identified and attempts were made to alter existing semi-empirical jet noise models to predict the noise originating from the laboratory scale nozzle.

Keywords: *jet noise, supersonic transport, LTO-cycle, LAPCAT II, STRATOFLY, hypersonics*

1. Introduction

The stratosphere is the highest layer in the atmosphere where aircraft can still fly. Nevertheless, it is presently rarely exploited for commercial aviation. As Europe's Vision for Aviation predicts globally a six-fold increase in passenger by 2050, flight levels above the troposphere become attractive and maybe the only way to realize this.

One of the challenges associated with the re-introduction of supersonic aircraft is the associated noise. The main issues thereto are the sonic boom and the jet noise originating from the propulsion system. The latter, which is the focus of this study, is particularly important during the LTO cycle due to the new types of engines that are being developed for supersonic aircraft. This research addresses jet noise generated during the (subsonic) take-off and landing phase of the LAPCAT II hypersonic transport aircraft that is studied within the EU-funded STRATOFLY project.

[1] *NLR (Royal Netherlands Aerospace Centre), 8316PR Marknesse, The Netherlands, karel.lammers@nlr.nl*
[2] *NLR (Royal Netherlands Aerospace Centre), 8316PR Marknesse, The Netherlands, remco.habing@nlr.nl*
[3] *VKI (von Karman Institute for Fluid Dynamics), B1640 Rhode-Saint-Genèse, grossir@vki.ac.be*
[4] *VKI (von Karman Institute for Fluid Dynamics), B1640 Rhode-Saint-Genèse, schram@vki.ac.be*

2. LAPCAT II propulsion system

2.1. Geometry

The propulsion system of the LAPCAT II aircraft consists of a dual-mode ramjet (DMR) for the hypersonic part of the flight trajectory and six air turbo rockets (ATR) located in 2 bypass ducts (3 ATR's in each bypass duct), as can be seen in Fig. 1. The bypass ducts and the DMR share one combined nozzle.

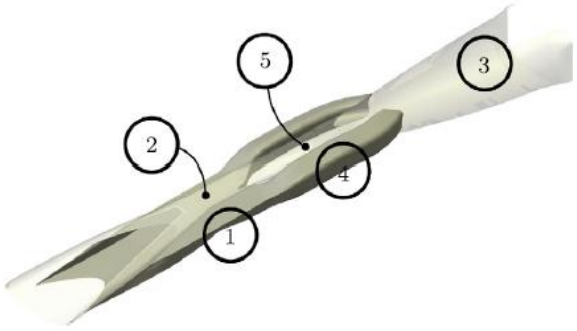

Fig. 1 LAPCAT II propulsions system: (5) DMR, (4) ATR bypass duct, (3) Combined nozzle. Picture reproduced from [ref. 1].

2.2. Nose-to-tail CFD

The propulsion system of the LAPCAT II vehicle consists of a complex nozzle. A nose-to-tail CFD analysis of this propulsion system has been performed by Krempus [ref. 2] for a range of operating conditions. In Fig. 2 - Fig. 5, flow fields obtained by Krempus are shown for two different flight speeds, both cases are for subsonic flight speeds occurring during take-off.

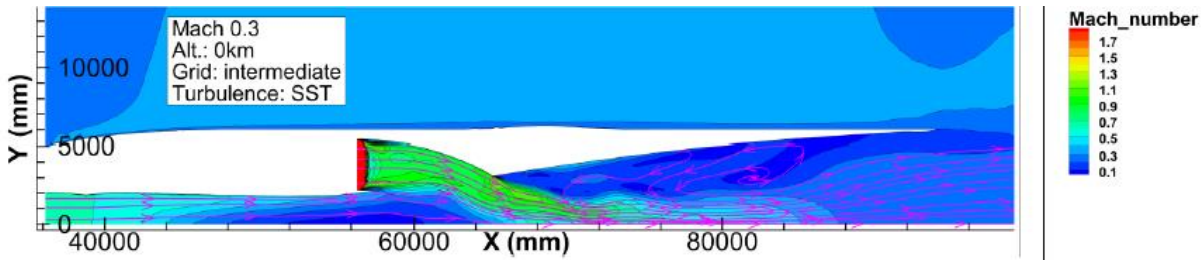

Fig. 2 Cross section of the flow field for 0.3 flight Mach number through the propulsion system, y=0 is the symmetry plane of the aircraft. The cross section is taken at a height corresponding to the centreline of the bypass ducts. Picture reproduced from [ref. 2].

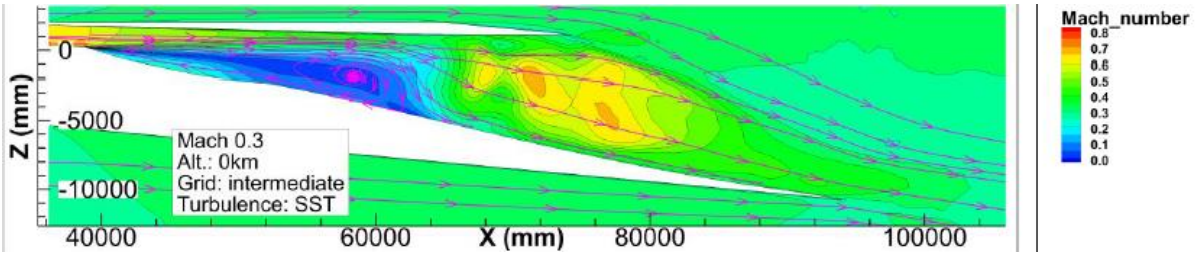

Fig. 3 Cross section of the flow field for 0.3 flight Mach number through the propulsion system at the symmetry line of the aircraft. Picture reproduced from [ref. 2].

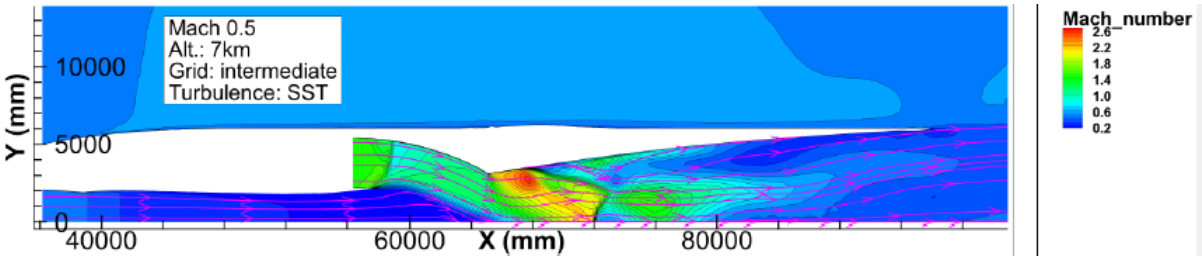

Fig. 4 Cross section of the flow field for 0.5 flight Mach number through the propulsion system, y=0 is the symmetry plane of the aircraft. The cross section is taken at a height corresponding to the centreline of the bypass ducts. Picture reproduced from [ref. 2].

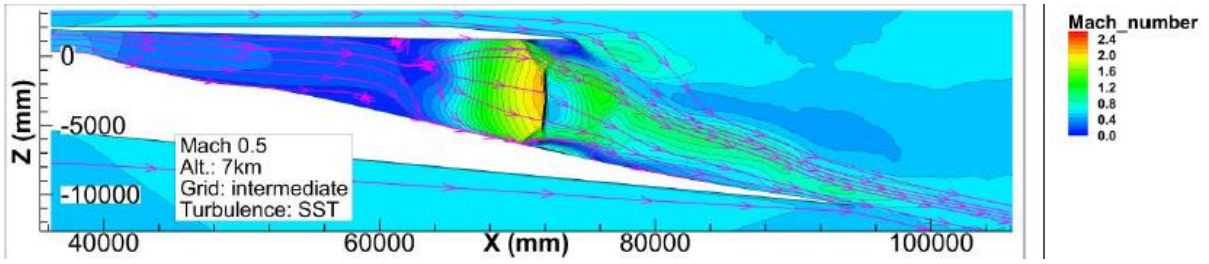

Fig. 5 Cross section of the flow field for 0.5 flight Mach number through the propulsion system at the symmetry line of the aircraft. Picture reproduced from [ref. 2].

On the basis of these CFD computations, some flow features are identified which are believed to be possible important noise sources. The following flow features observed within the nozzle system are believed to be relevant to the noise production problem:

- the impingement and merging of the two ATR bypass duct flows in the nozzle;
- the normal shock occurring downstream of that merging zone for some operating conditions;
- the mixing of the fully separated or wall attached jet in the combined nozzle.

The turbulent mixing of the subsonic jet discharging at the outlet of the combined nozzle is naturally another source of noise.

3. Simplified nozzle geometry

3.1. Design philosophy

To evaluate the jet noise mechanisms that are expected in the LAPCAT II aircraft propulsion system, experiments with a laboratory-scaled nozzle have been performed. These experiments are aimed at a better understanding of the effectiveness of the airframe integration in terms of noise reduction, and for the validation of a semi-empirical jet noise model that was developed in the STRATOFLY project (see section 5).

The highly three dimensional flow within the LAPCAT II propulsion system makes it quite complex to investigate experimentally, and hardly amenable to noise prediction based on a simplified, semi-empirical model. A more generic and simpler geometry has thus been considered as a first step, designed to reproduce the main physical mechanisms featured above on the basis of the CFD analysis of Krempus [ref. 2], but with the simplifications offered by an axisymmetric nozzle configuration. It was decided to replace the two lateral ATR nozzles by an annular nozzle, distributing the slightly supersonic flow across the full annulus.

3.2. Simplified nozzle

The outer contour of the annular nozzle follows an hyperboloid curve. The curvature radius at the nozzle throat is equal to 30mm. The divergent angle for the outer nozzle wall is set to 3 degrees. The subsonic convergent and the one appended to the nozzle both follow fifth order polynomials. This ensures continuity of the wall curvature all along the contour and minimizes the disturbances introduced

to the nozzle flow. A series of Navier-Stokes CFD simulations have been performed using a commercial code providing second order space accuracy. The k-ε turbulence model and a perfect gas equation of state are used. The test gas is dry air. Structured meshes with over 215 000 cells are used with mesh refinement along each wall. The stagnation pressure at the inlet of the inner and outer nozzles have been varied numerically independently from each other, as illustrated in Fig. 6 and Fig. 7 (with the contours of pressure and Mach numbers), showing that the axisymmetric coaxial nozzle designed is able to reproduce flow topologies resembling the ones shown in Fig. 2 - Fig. 5, without the need to alter the nozzle geometry.

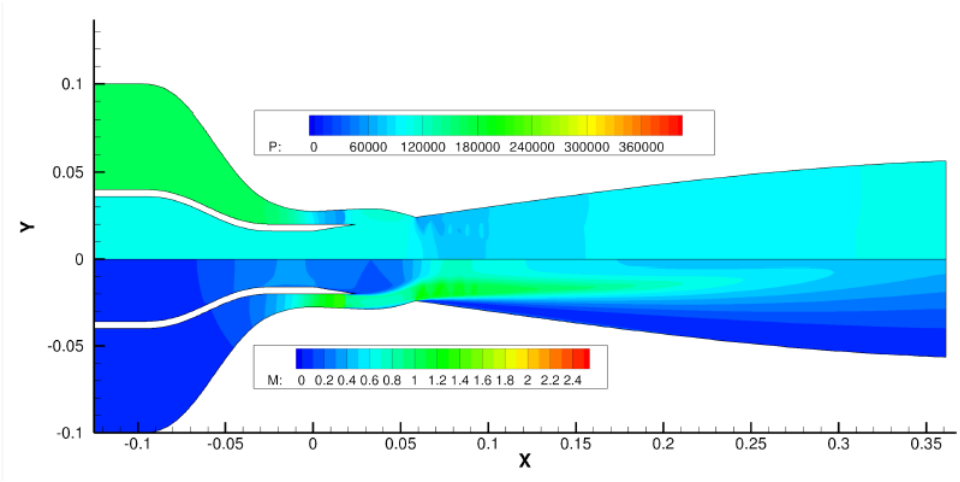

Fig. 6 Simplified axi-symmetric nozzle representing the flight Mach number 0.3 flow topology. Top-half: static pressure; bottom half: Mach number.

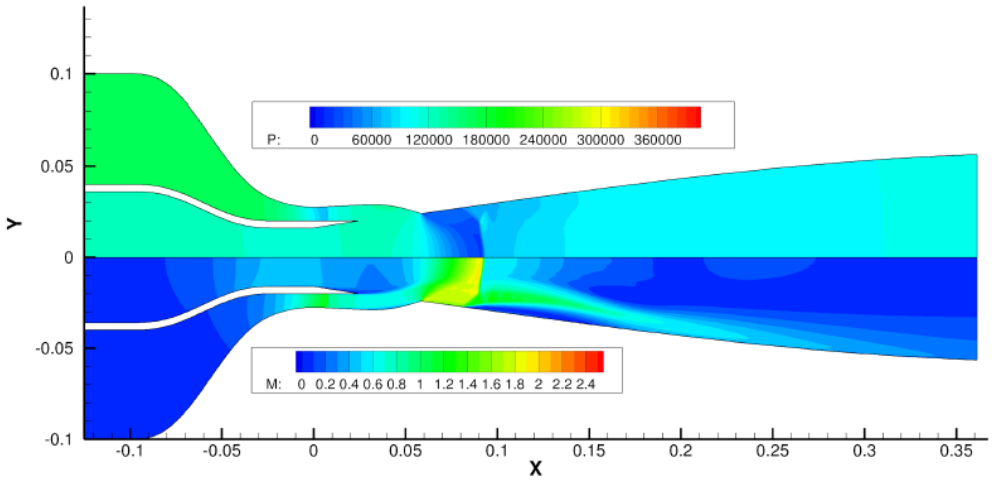

Fig. 7 Simplified axi-symmetric nozzle representing the flight Mach number 0.5 flow topology. Top-half: static pressure; bottom half: Mach number.

As can be seen, flow topologies similar to those calculated by Krempus have been obtained by varying the operating conditions. The key flow features identified in paragraph 2.2 seem to be present in the simplified nozzle as well. The nozzle contour provided by VKI formed the basis for the nozzle mechanical design and subsequent manufacture by NLR. In the remainder of this paper the simplified nozzle will be referred to as the STRATOFLY nozzle.

The conceptual design of VKI is converted into a physical nozzle by NLR. The nozzle section is divided into four sections, as shown in Fig. 8. Section #4, #3 and #2 can be removed to evaluate the effect of different stages of the nozzle. When only section #1 is installed, a coplanar nozzle is obtained. This configuration will be used to compare the experimental results against existing semi-empirical jet noise models used by NLR. With the convergent section #2, the effect of jet impingement can be evaluated. With section #3 and #4 the effect of shrouding the jet can be evaluated. From CFD computations

performed by VKI it was observed that shortening the shroud (only section #3) results in very different flow topologies, indicating that the shroud has not only an acoustic effect but also alters the flow. Noise measurements to evaluate the net effect of the shroud have been performed.

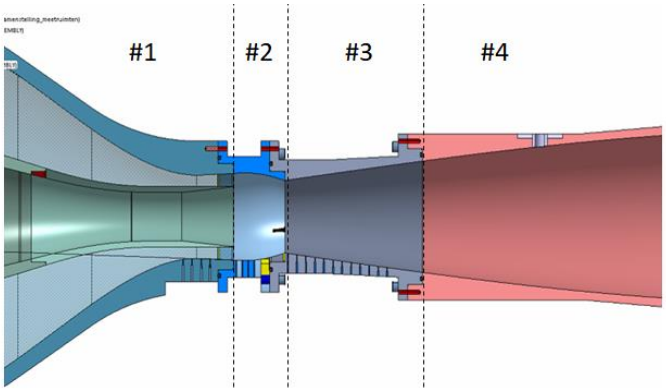

Fig. 8 Laboratory scale STRATOFLY nozzle.

4. Jet noise prediction model

4.1. Dual-stream jet noise model

A theory-based empirical model to predict jet noise was developed by J. R. Stone et al. [ref. 5]. The model covers single jets, dual stream jets with a conventional velocity profile and dual stream jets with an inverted velocity profile (IVP). The single jet model consists of two noise sources. These are the jet mixing noise and the shock noise. The mixing noise model consists mainly of theoretical relations which were determined by Lighthill and Ffowcs Williams [ref. 4]. For supersonic jets, shocks can form in the jet. These shocks are known to generate noise. The shock noise is determined using a theoretically-based model determined by Harper-Bourne and Fisher [ref. 3]. The shock waves in a choked jet are accountable for a source of broadband sound, often termed shock associated sound, and screech tones (narrow-band). Stone's model only includes shock associated sound, as typically screech is suppressed by an appropriate design for a nozzle.

The dual stream IVP jet noise model is based on that of the single stream circular jet noise model. The present research only focuses on the IVP jet noise prediction model, since for the subsonic part of the trajectory the ATR generates high velocity jets and the DMR acts like a flow-through channel. The jet noise for an IVP coaxial nozzle is considered to be made up of four constituent sources:

- Merged-jet / ambient mixing region
- Premerged-jet / ambient mixing region
- Inner-stream shock / turbulence interaction
- Outer-stream shock / turbulence interaction

The noise sources are assumed to be uncorrelated. Fig. 9 shows a schematic illustration of the typical IVP jet noise spectrum and sources.

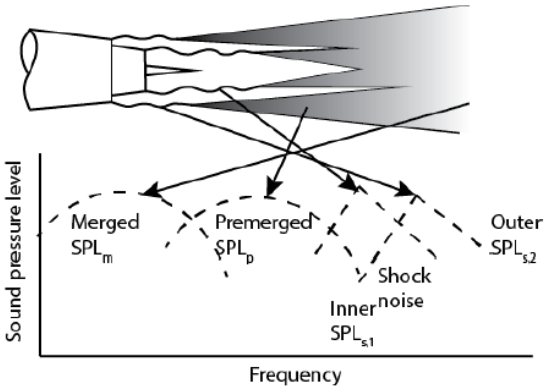

Fig. 9 Schematic overview of the four different noise sources in the IVP jet noise model.

More information about the jet noise model can be found in Stone's paper [ref. 5]. The implementation of this semi-empirical model for coaxial flow has been verified and validated within the STRATOFLY project, see e.g. [ref. 6, 7].

4.2. Duct propagation analogy

The purpose of the semi-empirical jet noise prediction model is to evaluate noise certification levels for a specified aircraft and flight path. To do so, the flight path is divided in small time steps and noise predictions are done for each timestep. To this extend an efficient and quick tool is desired, involving limited computational effort. Acoustic wave propagation in ducts is dominated by acoustic modes, where predicting acoustic radiation of these modes to the free field at the duct termination is a computational expensive process. Taking the application of the jet noise prediction tool into account, such a computational expensive process is not desirable. Instead the semi-empirical duct directivity model described by Day et al. seems to offer an attractive alternative [ref. 8]. Their work concerns the application of a chart for determining the directional properties of sound emitted from the open end of a ventilation duct. The directivity index chart from Day et al. is shown in Fig. 10. The chart shows the propagation effect as function of non-dimensional frequency for different directivity angles. Note that the directivity angles in the present research have been converted to a sign convention consistent with Stone's model. A positive directivity index means that the sound is amplified and a negative directivity index indicates sound attenuation.

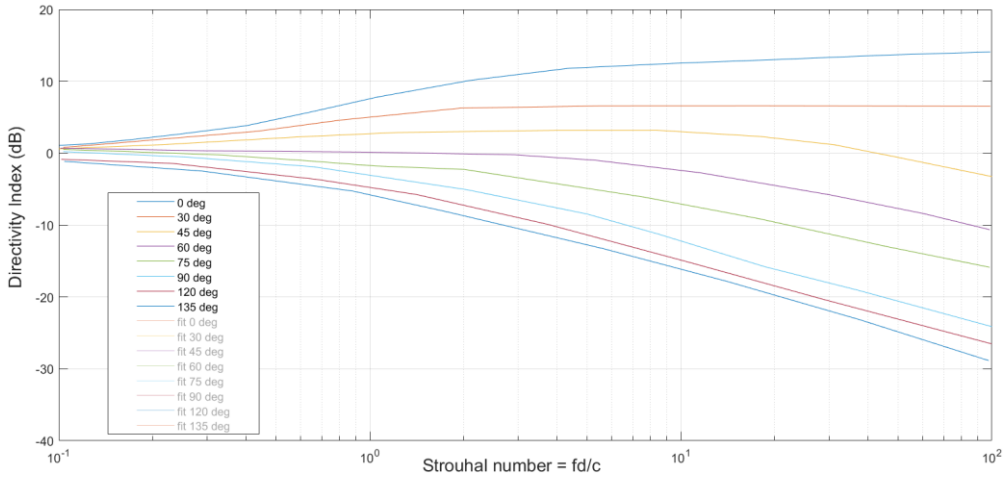

Fig. 10 Duct directivity index chart. Retrieved from Day et al. [ref. 8] (polar angle definition in this plot not yet converted to the definition consistent with present research).

This directivity index describes the directivity effect as function of frequency for an omnidirectional source. When the source strength of the sound source in the duct is known, the sound pressure level at a position in the free field around the open end of the duct can be simply calculated with the

directivity index [ref. 8]. The sound power can be calculated per frequency, by doing so the distribution of sound power per frequency of the internal sound source is maintained.

Looking at Fig. 10, it can be observed that for very low Strouhal numbers (< 0.2) the duct has negligible effect on the propagation of sound. Using the nozzle exit diameter of the laboratory STRATOFLY nozzle which is 112mm and the ambient speed of sound 346 m/s, the directivity effect for frequencies below 800 Hz is less than 2 dB and the sound pressure level follows simply from the sound power level taking geometrical spreading into account. The directivity effect of the duct becomes more apparent with increasing frequency. The highest frequency measured during the STRATOFLY experiments was 80 kHz, this corresponds to a Strouhal number of 26. For the downstream directivity angles (Stone's convention) between 135 degree and 180 degree it can be observed that the sound is amplified (especially for higher frequencies). For lower directivity angles the sound is attenuated (especially for higher frequencies and the most upstream directivity angles). This appeared to be a similar effect as observed in the STRATOFLY jet noise experiments, and founded the reason for application of the above mentioned duct propagation analogy.

5. Experimental investigations

5.1. Test set-up and instrumentation

The experiment has been performed in NLR's Aero-acoustic Wind Tunnel (AWT). Rather than using a closed- or open test section, the jet noise test-setup was conducted without operating wind tunnel. A dedicated nozzle supply system was developed and mounted at the tunnel contraction structure. The anechoic chamber has a volume of 8m x 9m x 5m, with a specified sound absorption coefficient of 99% for frequencies above 200 Hz.

In order to generate a dual-stream jet in the STRATOFLY nozzle, an external air supply system was rented. This system features a compressor, adsorption dryer, split piping with individual pressure regulators. A ventilation hatch in the AWT circuit was opened for venting and the contraction of the AWT was closed to prevent circulation. The upstream part of the modular STRATOFLY nozzle (Fig. 8) is connected to the dedicated supply unit, see left hand side of Fig. 11. The core duct includes a choke plate (which was removed during the 2nd test entry) enclosed by metal foam plates, a total pressure and temperature sensor in a settling environment and turbulence screens to improve the flow quality before being accelerated into the STRATOFLY nozzle part. The metal foam plates are used to enable sound absorption of the supply line noise, choke plate induced noise and nozzle reflected noise (preventing standing waves). The annular outer duct also includes metal foam disks to homogenize the dual radial incoming flow and enable supply line spurious noise damping. The outer duct is also instrumented with a total pressure and temperature sensor. The core duct is fixed to the outer duct upstream of the turbulence screens by 3 NACA0010 profile shaped struts.

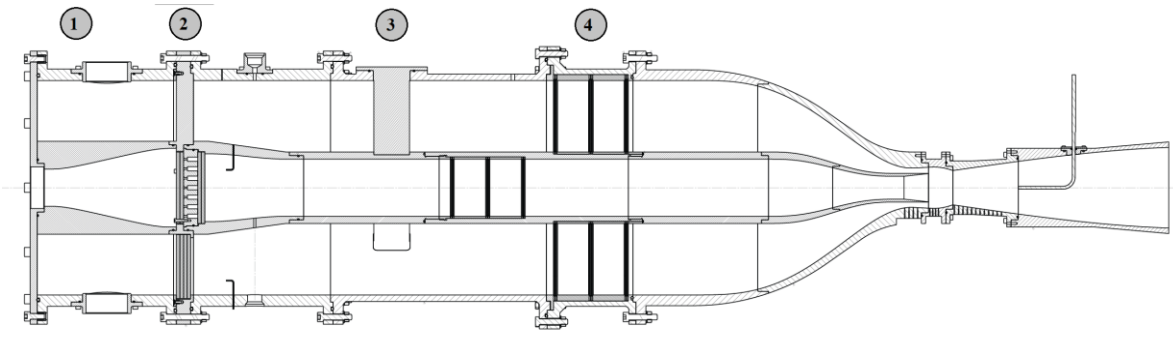

Fig. 11 Design of pressurized air system for dual-stream jet generation at STRATOFLY nozzle.

The dual stream nozzle jet Mach numbers can be controlled individually by using two remote controlled pressure regulators for the air supply lines. The jet Mach number can be derived by measuring the supply total pressure and applying isentropic flow relations. In case of a coplanar nozzle it is assumed that the jet static pressure equals the measured ambient static pressure. In case of the STRATOFLY nozzle with modular parts mounted (Fig. 8 with section 2, 3 or 4) The static pressure can also be obtained from measurement of static wall pressures. The taps in section 1 are used to check the presence of chocked flow, in section 2 to evaluate the Mach number of the inner jet in case of jet-jet

interaction (CFD results indeed suggest that the related static pressure is only a weak function of radial position), in section 3 to allow checking for shock generation in the nozzle shroud. The shroud also includes a provision for traversing a Pitot-static tube.

In order to measure the acoustic far-field, a minimum distance from noise source to the microphone positions is required. This minimum depends on the type of jet (i.e. subsonic, supersonic cold, supersonic heated and single versus dual-stream jet) [ref. 9, 10]. The present test set-up only allows cold/unheated jet testing where the geometry based far-field requirements are met. The nozzle suspension can be traversed in flow direction to keep the nozzle exit plane fixed in space for all nozzle configurations. The microphone array consists of 11 ¼" free-field microphones that are mounted on fixed poles and set a normal incidence to the nozzle exit. The vertical and horizontal support rods are acoustically treated. The microphones are placed at equidistant polar angles of 10 deg in the range of 50 – 150 deg. The protective grids of the microphones are removed to prevent internal resonances and the factory frequency response fit curves are implemented to yield a flat response up to 100 kHz. In order to allow for anechoity checks, additional microphones are installed at various lateral positions. The acoustic data is acquired by a 16 bit multi-channel dynamic data acquisition system. The data post-processing included microphone sensitivity correction, atmospheric absorption correction and geometric spreading correction to yield SPL spectra at a reference distance.

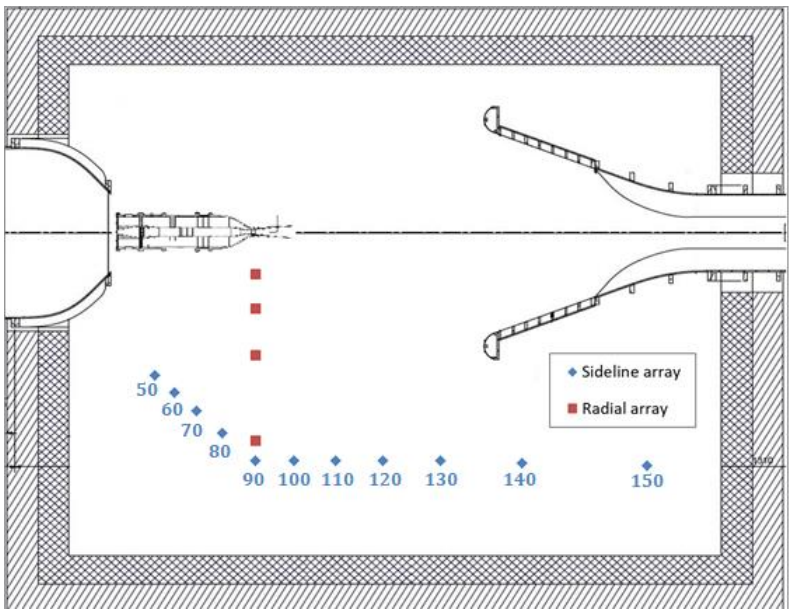

Fig. 12 Sketch of test set-up with sideline microphone array in NLR-AWT anechoic room (top view).

5.2. Preliminary measurements

Preliminary jet noise measurements with the STRATOFLY nozzle have been performed in the NLR-AWT in September 2019 and the second test in this facility was completed in August 2020. An extensive data quality evaluation for the acoustic dataset measured at NLR was performed. In order to assess the quality of the data that was measured during the acoustic tests, the following aspects were evaluated:

- Axisymmetric velocity profile check (only pre-test)
- Acoustic data corrections and anechoic room check
- Repeatability check
- Metal foam effect evaluation (only pre-test)
- Signal to Noise Ratio (SNR) check
- Resonances evaluation
- Evaluation of acoustic coherence
- Comparison of measured wall pressures against CFD results
- Convergent nozzle single jet measurements compared with noise predictions

The microphone array for measuring directivity effects is located at one lateral side. Assuming that the jet is axi-symmetric, makes the measured directivity effect applicable to all azimuthal angles around

the centerline of the nozzle. To evaluate this assumption flow velocity measurements were performed to check symmetry of the jet. These flow measurements were performed during the pre-test only and indicated a symmetric and robust jet.

With the radial acoustic array, anechoic conditions can be evaluated. The anechoic room is designed to absorb the noise generated by the source (i.e. jet), thereby avoiding reflections and acoustic interference. If this is the case, the sound pressure amplitude should decrease inversely proportional with distance between the source and the microphone head. Additionally, acoustic energy is absorbed by the medium in which the acoustic waves travel. For the typical audible frequency range this is a negligible effect within the dimensions of the anechoic room. However, for higher frequencies (due to model scale) this can have a significant effect and should be taken into account in the evaluation of the anechoic properties of the room. The data is corrected for geometric spreading and atmospheric damping according to ISO 9613. The corrected SPL spectra collapse well (< 1 dB), showing proper anechoic conditions in the third-octave band frequency range [315 Hz, 80 kHz].

A typical repeatability of 1 dB up to 80 kHz was found for the broadband jet noise spectra.

During the pre-test some issues related to SNR and resonances were identified. The SNR issue was related to cable shielding induced high electrical background noise levels. The resonances issue was related to both laminar flow and nozzle exit axi-symmetry induced acoustic modes. During the 2nd test entry the measures for solving these issues were found to be successful.

Besides the acoustic data, wall pressures were also measured to evaluate consistency between the VKI Navier-Stokes CFD simulations and the actual realized nozzle. Fig. 13 shows two comparisons between CFD and pre-test experimental data. The abrupt increase in static pressure suggests the existence of i) choked outer flow, ii) normal shock in the shroud, (compare Fig. 2 - Fig. 5). The good agreement allows interpretation of the flow by CFD and coupling of predicted flow quantities to the semi-empirical jet noise model.

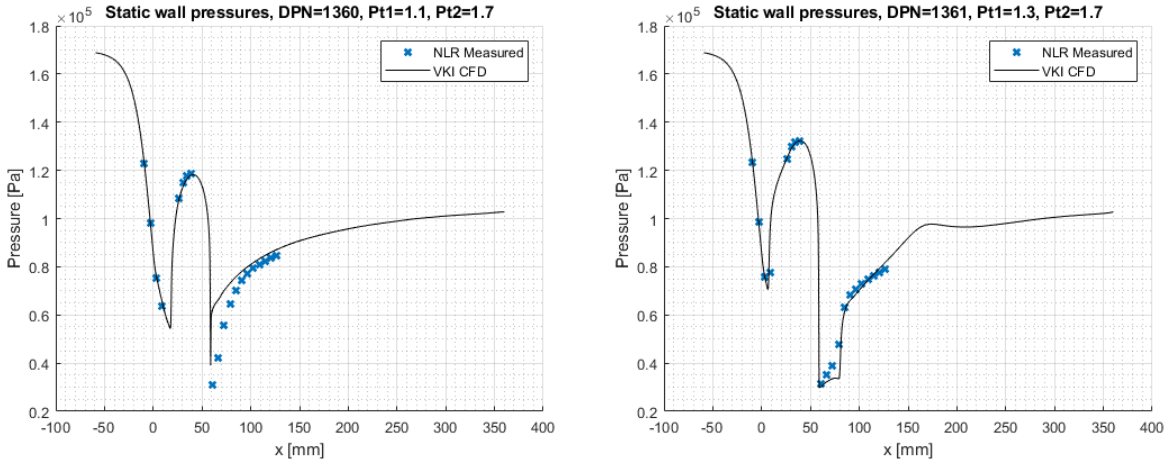

Fig. 13 Comparison of wall pressures: CFD vs. experimental results. Left is for the flight Mach number 0.3 flow topology and right for the flight Mach number 0.5.

Finally, besides convergent inner nozzle single stream jet noise checks (with specially designed nozzle exit insert part) also single pressurized duct measurements were performed. If the noise originating from the STRATOFLY nozzle is dominated by subsonic jet noise, the sound power level should scale with the power 7.5 as function of jet velocity. The evaluation of the sound power level scaling law when i) only the inner jet is operated and ii) only the outer jet, revealed that the jet mixing is indeed the dominant noise source (for subsonic flows). This was also confirmed by the data collapse of the measured noise spectra when the SPL is divided by $(U_j^{7.5}\rho D^2)/c^5$ and plotted against the Strouhal number. Where U_j is the jet velocity, ρ is the ambient density, D is the nozzle diameter and c is the ambient speed of sound.

5.3. Test program

In the remainder of the present paper the experimental jet noise results from the second test entry (i.e. improved SNR and suppressed parasitic tonal noise components) have been used. The test program of the second entry included the following nozzle configurations and conditions:

- Configurations: variation of resonance preventing inserts, coplanar, coplanar & convergent part, coplanar & convergent part & short shroud, coplanar & convergent part & short shroud & full shroud
- Conditions: repeat reference single / dual stream, variations in combinations inner- and outer-jet Mach nr. ($0 \leq M_{in} \leq 1.5$ and $0 \leq M_{out} \leq 1.4$), variations in combinations inner- and outer- jet total pressure ($1.1 \leq Pt_{in} \leq 1.7$ and $1.7 \leq Pt_{out} \leq 2.8$ bar)

5.4. Jet noise comparison results

To make the analysis and modelling of the noise originating from the STRATOFLY nozzle more manageable, the analysis focussed on two flight conditions and two directivity angles. These concern the following conditions and directivity angles:

- Directivity angle 50 deg

  For supersonic jets, shock noise will be mainly present in the upstream directivity angles.

- Directivity angle 140 deg

  Mixing noise will dominate in this downstream directivity angle range.

- Flight Mach number $M_f = 0.3$

  For this condition the core duct is supplied with 1.1 bar compressed air and the outer duct is supplied with 1.7 bar of compressed air. Comparison of noise predictions against experimental results for all measured directivities angles.

- Flight Mach number $M_f = 0.5$

  For this condition the core duct is supplied with 1.3 bar compressed air and the outer duct is supplied with 1.7 bar of compressed air. Comparison of noise predictions against experimental results for all measured directivities angles.

In order to evaluate the measured STRATOFLY nozzle jet noise characteristics, five different prediction methods have been applied. The first modelling approach follows the unaltered Stone's model for IVP jets (method 1). The second method uses the same noise source and directivity modelling, but the required input parameters are derived from CFD simulations (method 2). The third method shows the analogy with a duct propagation model (method 3). Subsequently, this duct propagation model is coupled to Stone's IVP model with input derived from CFD, where Stone's model is only used for the source power description and the duct model prescribes the directivity (method 4). And in the last method some assumptions are made about the flow topology (which are based on the CFD simulations). These assumptions make it possible to use the model for a noise impact study for a prescribed flight path without having the necessity to perform a CFD simulation for each timestep along the flight path (method 5). The comparison plots include the results of all prediction methods, but will be explained step by step.

The measured jet noise spectra are depicted as orange curves in Fig. 15 - Fig. 16. The directivity plots are presented as overall SPL vs. polar angle in Fig. 17. As a first attempt to understand the measured directivity and spectra of the STRATOFLY nozzle (i.e. full shroud), a comparison is made with noise predictions from the unaltered Stone's model for IVP jets. As input for the predictions, the jet conditions have been derived from the measured total quantities in the supply unit per duct, ambient static pressure and assuming isentropic flow. Since the predicted jet remains subsonic, no shock noise component is present (black curve in Fig. 15 - Fig. 17). The predictions underestimate the jet noise levels. For the upstream directivity angle there seems to be a mismatch in the shape of the spectrum for the lower frequencies. The discrepancy between the experimental results and predictions is not unexpected, since the STRATOFLY nozzle clearly has an aerodynamic effect.

Looking at the CFD results for the laboratory nozzle it can be observed that for these operating conditions the flow coming from the ATR duct merges in the combined nozzle and forms a new high speed separated jet in the combined nozzle (Fig. 6). This is the jet that will finally mix with ambient conditions. So in terms of mixing noise, the jet conditions at a plane downstream of the contraction part is taken from the CFD results as input for Stone's model. Due to the increased jet velocity, the sound pressure level over the complete spectrum increases compared to the previous simulation (green curve Fig. 15 - Fig. 17). Since the jet is now supersonic, the shock noise component in the spectrum of the upstream directivity angle can be clearly observed. However, this increase in high frequency noise is absent in the experimental spectrum and there is a fundamental mismatch in the shape of the spectrum. Looking at the downstream directivity angle, the agreement between the predicted spectrum and the measured spectrum seems reasonable but there is still an underestimation in the high frequency domain.

As a first attempt to check if the semi-empirical duct directivity model can be used to model the directivity effect of the STRATOFLY nozzle, the model is applied in combination with an arbitrary omnidirectional sound source with a tuned sound power level of 115 dB for M_f=0.3 and 112 dB for M_f=0.5 (pink curve in Fig. 15 - Fig. 17). A good agreement between the tuned curves and measurements can be obtained. This formed the base for further development steps.

As next step the duct propagation model is coupled to the jet noise prediction model of Stone, see Fig. 14. For the jet noise spectral power prediction step the input is based on CFD computations. Due to the duct termination directivity the acoustic energy of the sound source is directed to downstream angles and this effect becomes stronger with increasing frequency.

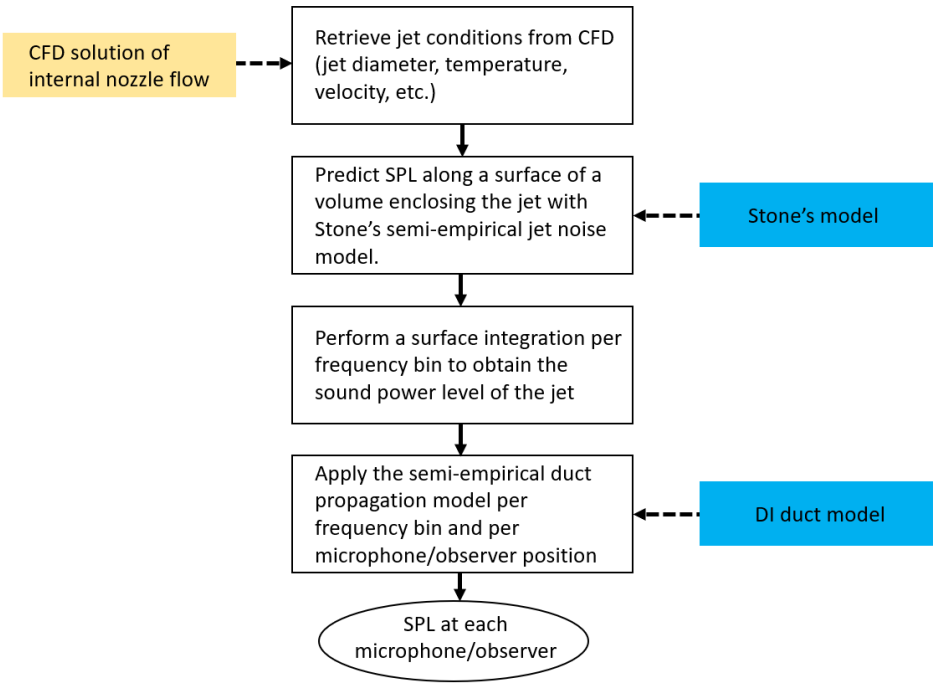

Fig. 14 Schematic view of modelling STRATOFLY nozzle jet noise with CFD input (method 4).

The prediction results are shown in Fig. 15 - Fig. 17 (blue curves). As expected the high frequency shock noise is directed to downstream directivity angles due to the propagation effect of the shrouding nozzle. In general, a reasonable agreement in SPL spectra can be found between these predictions and measurements. In general, the shape of the directivity pattern seems to be in agreement with the measured directivity pattern, but there seems to be a systematic underprediction of 4 to 10 dB in OASPL.

Ideally, the necessity of using CFD to generate input for the noise prediction step is avoided. To that extent a final modelling approach was explored. To that aim following assumptions were made based on observations of the CFD flow topology: i) the core flow and outer flow do not mix upstream of the contraction plane, ii) there are no losses in the outer flow stream annulus and it does not change in

total cross-sectional area, therefore the core stream reduces in diameter, iii) the jet Mach number of the outer flow is assumed to be equal to the design Mach number of the outer nozzle in coplanar configuration. With this procedure the jet in the STRATOFLY nozzle is modelled as an equivalent IVP jet. The prediction results are shown in Fig. 15 - Fig. 17 (red curves). In general, the OASPL is now systematically overpredicted by 3 to 6 dB.

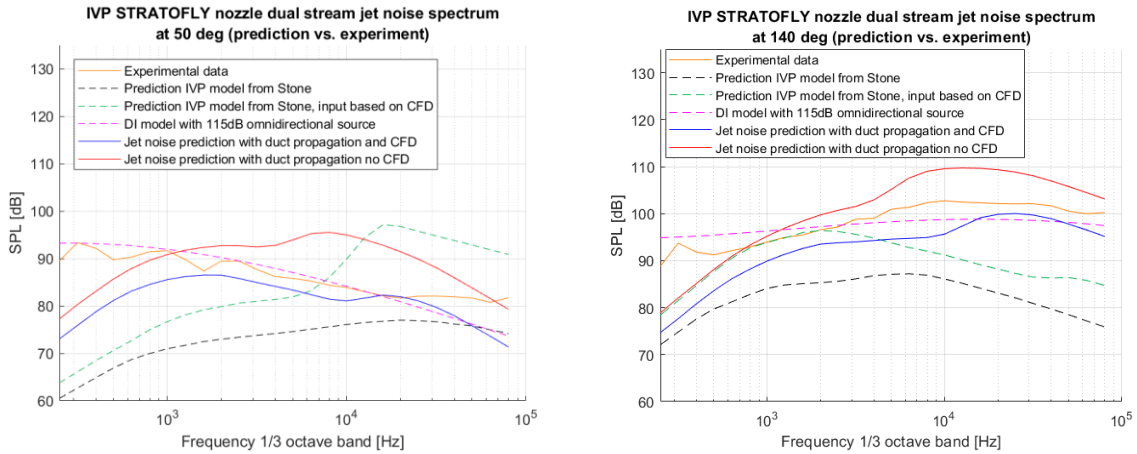

Fig. 15 Comparison of measured and predicted jet noise spectra for M_f=0.3.

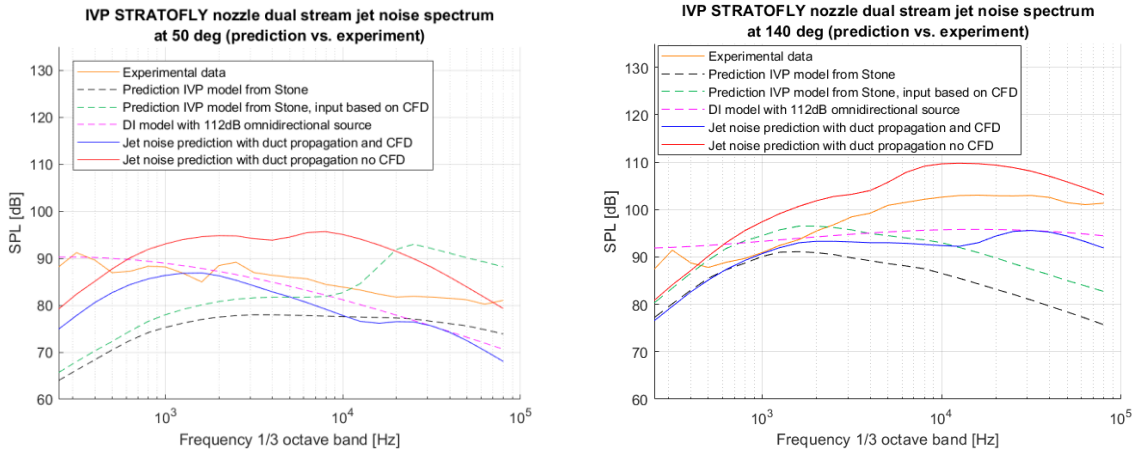

Fig. 16 Comparison of measured and predicted jet noise spectra for M_f=0.5.

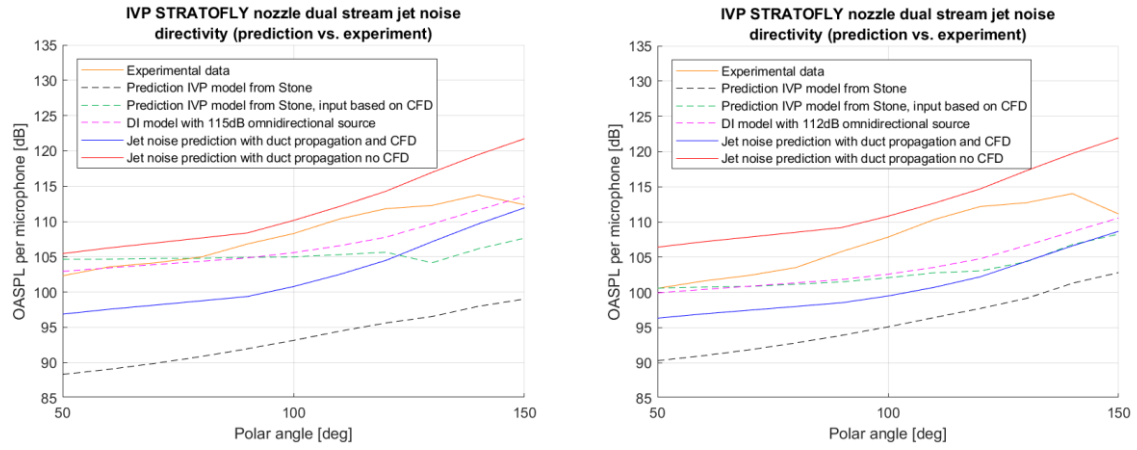

Fig. 17 Comparison of measured and predicted jet noise directivity (left: M_f=0.3, right: M_f=0.5).

6. Conclusions

The jet test rig and nozzle that were specifically designed for the STRATOFLY project are working properly. The laboratory scale nozzle, designed by VKI, is able to capture key noise source mechanisms identified based on full scale CFD simulations, by simply changing the operating conditions. A good agreement in static wall pressures between CFD predictions and experimental wall pressures is found. This makes it possible to couple flow topology information from VKI's CFD solutions to NLR's noise predictions with semi-empirical jet noise models. The noise prediction is built upon the modelling of an equivalent jet inside the STRATOFLY nozzle by using Stone's semi-empirical jet noise model for IVP jets.

Aerodynamic effects of the STRATOFLY nozzle cannot be neglected for noise predictions. The aerodynamic effect can be taken into account by incorporating flow topology information from CFD calculations. Besides the aerodynamic effect, the most dominant acoustic effect is that the STRATOFLY nozzle directs more acoustic energy towards downstream directivity angles. This effect becomes stronger with increasing frequency. Looking at the measured spectra and the flow topology from CFD results for flight Mach number 0.3, there is a strong analogy with a sound source in a duct radiating to free field conditions at the open end of the duct. Therefore, the noise from the STRATOFLY nozzle was predicted by coupling Stone's semi-empirical jet noise model to a duct propagation model. The jet noise model provides spectral information and sound power levels. But the typical jet noise directivity pattern is replaced by the duct propagation model. In this process the input for Stone's semi-empirical jet noise model can be either taken directly from CFD results or can be derived via isentropic flow relations in combination with some assumptions of the flow topology. For a noise impact study, the latter is more desirable since CFD results are not required for each point along the flight path.

The method that uses jet conditions from CFD directly results in a typical underprediction of 4 to 7 dB in OASPL for each directivity angle, but can also be as large as 10 dB. This accuracy is to some extent related to the engineering judgement that is involved when acquiring the input data from CFD. The method that derives the jet conditions via isentropic relations in combination with some assumptions of the flow topology is slightly more accurate and results in a typical overprediction of 3 to 6 dB in OASPL for each directivity angle. This overprediction is likely to be related to the neglection of losses and mixing in the annular stream tube. Therefore, it is believed that the overprediction will be smaller when aerodynamic losses are smaller at the region where the ATR jet interacts with the DMR flow. Overall the agreement between the experimental and predicted SPL spectra is reasonable for this cold jet set-up. Stone's semi-empirical jet noise model is also applicable to hot jets and since the directivity effect of the duct propagation model is only related to the duct geometry, the method reported in this work may also be applicable to hot jets although this has not been confirmed.

7. Acknowledgments

The H2020 STRATOFLY Project has received funding from the European Union's Horizon 2020 research and innovation programme under grant agreement No 769246.

8. References

1. Fernández-Villace, V., Paniagua, G., & Steelant, J. (2014). Installed performance evaluation of an air turbo-rocket expander engine. *Aerospace science and technology*, 35, 63-79.
2. Krempus, D. (2017). Evaluation of the Aero-propulsive Performance of a Hypersonic Aircraft during the Acceleration Phase. (Unpublished master thesis). *Institut für Thermodynamik der Luft- und Raumfahrt der Universität Stuttgart*, Stuttgart, Germany.
3. Harper-Bourne, M. (1974). The noise from shock waves in supersonic jets-Noise Mechanism. Agard Cp-131.
4. Stone, J. R., & Montegani, F. J. (1980). An improved prediction method for the noise generated in flight by circular jets. *NASA* TM 81470.
5. Stone, J., Zola, C., & Clark, B. (1999). An improved model for conventional and inverted-velocity-profile coannular jet noise. In *37th AIAA Aerospace Sciences Meeting and Exhibit* (AIAA-99-0078).

6. Habing, R. (2019). Development of an improved jet noise prediction model; From single stream to conventional and inverted velocity profile coaxial jet noise. (Unpublished NLR report). *Netherlands Aerospace Centre*, NLR-CR-2018-511.
7. Thije, J. (2019). Validation of a semi-empirical dual stream inverted velocity profile jet noise prediction model. Master thesis. *University of Twente*, ME-328.
8. Day, A., Hansen, C., & Bennett, B. (2009). Duct directivity index applications. In *Acoustics Australia*, 37 (3), p.93.
9. Viswanathan, K. (2010). Distribution of noise sources in heated and cold jets: are they different? *Int. J. Aeroacoustics*, 9(4-5), 589-625.
10. Viswanathan, K. (2011). True farfield for dual-stream jet noise measurements. *AIAA J.*, 49(2), 443-447.